Scanning tunneling microscopy theory for an adsorbate: Application to adenine adsorbed on a graphite surface

Hui Ou-Yang, R. A. Marcus, and Bruno Källebring
Arthur Amos Noyes Laboratory of Chemical Physics,[a] *California Institute of Technology, Pasadena, California 91125*

(Received 19 January 1994; accepted 3 February 1994)

An expression is obtained for the current in scanning tunneling microscopy (STM) for a single adsorbate molecule. For this purpose the "Newns–Anderson" treatment (a "discrete state in a continuum" treatment) is used to obtain wave functions and other properties of the adsorbate/substrate system. The current is expressed in terms of the adsorbate–tip matrix elements, and an effective local density of states of the adsorbate/substrate system, at the adsorbate. As an example, the treatment is applied to the STM image of adenine adsorbed on a graphite surface, and the results are compared with experiment. The dependence of the image on the position of adenine with respect to the underlying graphite is considered. A discussion is given of the type of experimental STM data needed for suitable comparison of theory and experiment. In an analysis of the calculations, the role of each atom, its neighbors, next nearest neighbors, etc., in an adsorbed molecule is considered. The need for using in the present calculation more orbitals than only the HOMO and the LUMO of the adsorbate is also noted.

I. INTRODUCTION

Scanning tunneling microscopy (STM) is widely used to obtain images of bare surfaces[1] and of various atoms[2] and molecules[3] adsorbed on surfaces. The STM image of an adsorbate can provide information about the electronic structure of the adsorbate and about its interaction with the underlying substrate.

A theoretical treatment of STM going beyond bare surface was given by Lang, who considered a STM image of a single atom adsorbed on a sample surface.[4] He found that the STM images differed for chemically different atoms and that the STM pattern for a low-bias voltage images the Fermi-level local density of states of the sample at the position of the tip. In the case of Xe adsorbed on a Ni (110) surface, the normal tip displacement vs lateral tip displacement curve was calculated by Eigler *et al.* from the theory of Lang and they noted that it was in good agreement with experiment.[5]

In an early attempt to understand the STM image of a molecule adsorbed on a surface, Lippel *et al.* calculated the electron density distribution of the highest occupied orbital (HOMO) and that of the lowest unoccupied orbital (LUMO) of the isolated adsorbate and found a similarity between the orbital electron density and the STM image of the adsorbate.[6] In their calculation the adsorbate–substrate interaction was not included. Examples of other calculations on the interpretation of the STM images of adsorbate molecules are given in Refs. 7–11.

In a previous paper we formulated a theoretical treatment of STM and used it to treat images of bare surfaces of graphite and Au (111).[12] In the present paper this treatment is adapted to STM images of adsorbates, by introducing the Newns–Anderson treatment[13,14] for the wave functions and other properties of the adsorbate/solid substrate system. The STM image of the adsorbate is then related to an effective local density of states at the adsorbate and to the adsorbate–tip Hamiltonian matrix elements.

The theoretical treatment is given in Sec. II, and is applied to the STM image of adenine on a graphite surface in Sec. III, where the results and the comparison with the experimental STM image[15] are discussed. Concluding remarks and the type of further experimental data needed to facilitate comparison with theory are given in Sec. IV.

II. THEORETICAL MODEL

In the limit of low-bias voltage v, the net STM current from a commonly used transition metal tip such as tungsten or platinum to a sample in the absence and presence of adsorbates was given in Ref. 12 by

$$I=2e^2v[(2\beta)^2-(\mu_t-\alpha)^2]^{1/2}/\hbar(2\beta)^2 \times\sum_n\sum_m\int d\mathbf{k}_s|\langle d_m^t|H|\phi_{n\mathbf{k}_s}\rangle|^2\delta(\epsilon_s), \quad (1)$$

when the tip was treated as a semi-infinite linear chain of atoms. The d_m^t denotes the mth d orbital of the first tip atom (the atom closest to the sample), $\phi_{n\mathbf{k}_s}$ is the wave function of the adsorbate/substrate system with band index n and wave vector $\mathbf{k}_s$, and μ_t is the chemical potential of the tip. The parameters α and β are defined as $\alpha=\langle d_m^j|H|d_m^j\rangle$ and the average value of $\beta_m=\langle d_m^j|H|d_m^{j+1}\rangle$, respectively, with d_m^j denoting the mth d orbital on the site j of the tip. For notational brevity, the energy of the latter state $\epsilon_n(\mathbf{k}_s)$ has been written as ϵ_s. As an approximation, only the matrix elements between the adsorbate/substrate system and the atomic orbitals d_m^t of the first tip atom have been included. The more general expression for higher biases is given in Ref. 12. It is also straightforward to include the direct matrix elements between the tip and the substrate.

In the case of a sample being a bare substrate such as graphite, the relevant properties needed for Eq. (1), such as

[a]Contribution No. 8777.

 0021-9606/94/100(10)/7814/11/$6.00

the wave functions $\phi_{n\mathbf{k}_s}$, were obtained earlier.[16] They were used[12] in conjunction with Eq. (1) to calculate the STM image of graphite.

In the case of a system containing a single molecule adsorbed on a substrate, the electronic state for this system $\phi_{n\mathbf{k}_s}$ may be written as a linear combination of a molecular orbital state (or atomic orbital, in the case of a single atom) of the adsorbate ϕ_a and the orbital states of the substrate $\phi_{n\mathbf{k}_g}$

$$\phi_{n\mathbf{k}_s}=a_n\phi_a+\int d\mathbf{k}_g\, b_{n\mathbf{k}_g}\phi_{n\mathbf{k}_g}. \tag{2}$$

For simplicity of presentation, it is assumed in Eq. (2) that there is only one molecular orbital of the adsorbate involved in tunneling, but additional orbitals are included later and indeed are important.

Equation (2) for $\phi_{n\mathbf{k}_s}$ is next introduced into Eq. (1) and we then obtain

$$I=2e^2v[(2\beta)^2-(\mu_t-\alpha)^2]^{1/2}/\hbar(2\beta)^2 \times\sum_m |\langle\phi_a|H|d_m^t\rangle|^2\rho_{a,0}, \tag{3}$$

where

$$\rho_{a,0}=\sum_n\int d\mathbf{k}_s|a_n|^2\delta(\epsilon_s). \tag{4}$$

which serves, at the Fermi level energy ($\epsilon_s=0$) of the adsorbate/substrate system, as an *effective* local density of states of that system at the adsorbate. In the Newns–Anderson model,[13,14] the adsorbate state ϕ_a is treated via Eq. (2) as a "discrete state in a continuum," the states $\phi_{n\mathbf{k}_g}$ of the solid forming the continuum. Using the Newns–Anderson description, this $\rho_{a,0}$ is given by[13,14]

$$\rho_{a,0}\equiv\sum_n\int d\mathbf{k}_s|a_n|^2\delta(\epsilon_s)=\frac{\pi^{-1}\Delta_{a,0}}{(\epsilon_a+\Lambda_{a,0})^2+\Delta_{a,0}^2}. \tag{5}$$

Here $\epsilon_a=\langle\phi_a|H|\phi_a\rangle$ and is relative to the Fermi level of the adsorbate/substrate system. The half-width $\Delta_{a,0}$ and the effective energy shift $\Lambda_{a,0}$ are given by

$$\Delta_{a,0}=\pi\sum_n\int d\mathbf{k}_g|\langle\phi_a|H|\phi_{n\mathbf{k}_g}\rangle|^2\delta(\epsilon_g), \tag{6}$$

and

$$\Lambda_{a,0}=-P\sum_n\int d\mathbf{k}_g|\langle\phi_a|H|\phi_{n\mathbf{k}_g}\rangle|^2/\epsilon_g, \tag{7}$$

where the $\epsilon_g(\mathbf{k}_g)$ denotes the eigenvalues of the unperturbed substrate states $\phi_{n\mathbf{k}_g}$, and P denotes the principal part of the integral.

If there are several orbitals of the adsorbate involved in tunneling, we next make the approximation of summing over the contributions from the individual orbitals a of the adsorbate. That is, each orbital a is treated as interacting individually with the continuum of states in the solid ("nonoverlapping resonances")

$$I=2e^2v[(2\beta)^2-(\mu_t-\alpha)^2]^{1/2}/\hbar(2\beta)^2 \times\sum_{a,m}|\langle\phi_a|H|d_m^t\rangle|^2\rho_{a,0}. \tag{8}$$

This assumption is valid if the resonances indeed are not overlapping, namely, if the spacing between the adsorbate levels ϵ_a is appreciably larger than the width of the broadened levels $2\Delta_{a,0}$. Calculated values of these two quantities are compared in a later section as a test of this approximation.

It is seen from Eq. (8) that at the low-bias voltages used in Eq. (1), the STM image in the presence of an adsorbate depends upon $\rho_{a,0}$, evaluated at the Fermi level of the substrate/adsorbate system, and on the tip–adsorbate Hamiltonian matrix elements $|\langle\phi_a|H|d_m^t\rangle|^2$, summed over the adsorbate orbitals a and over the atomic orbitals d_m^t of the nearest tip atom. If a molecular orbital ϕ_a is written as the linear combination of real atomic orbitals, $\phi_a=\sum_{i=1}^N c_i^a f_i$, then the $\Delta_{a,0}$ in Eq. (6) becomes

$$\Delta_{a,0}=\pi\sum_{i,j=1}^N\sum_n c_i^a c_j^a\int d\mathbf{k}_g\langle f_i|H|\phi_{n\mathbf{k}_g}\rangle \times\langle\phi_{n\mathbf{k}_g}|H|f_j\rangle\delta(\epsilon_g), \tag{9}$$

where c_i^a denotes the coefficient of the ith atomic orbital f_i in the isolated molecular orbital ϕ_a and N is the number of atomic orbitals employed to form the molecular orbital.

Whereas the overall brightness of the adsorbed molecule depends on $\rho_{a,0}$, it is seen from Eq. (8) that the relative brightness of the individual atoms depends mainly on the term containing the tip matrix elements $\Sigma_m|\langle\phi_a|H|d_m^t\rangle|^2$. The latter can be written as

$$\sum_m|\langle\phi_a|H|d_m^t\rangle|^2=\sum_{i,j=1}^N\sum_m c_ic_j\langle f_i|H|d_m^t\rangle\langle d_m^t|H|f_j\rangle. \tag{10}$$

Equations (8)–(10) are used in the next section to calculate the STM image of adenine adsorbed on graphite.

III. RESULTS AND DISCUSSION

A. STM calculations: Common aspects

STM experiments have been used to obtain an image of adenine adsorbed on a graphite surface.[15] In these experiments an array of adenine molecules was observed on the graphite surface. In each STM image, the nitrogen atoms at the N_6, N_7, and N_9 positions in Fig. 1 did not appear, but N_1, N_3, and all C's did appear. In this experimental study the detailed geometrical structure of the array relative to the geometry of the underlying graphite lattice was not precisely determined, though some experimental constraints on the registry of the two lattices were obtained and are noted later.

The STM tip used for the experiment was Pt–Ir (90% Pt). In the following calculations, the tip is approximated as above as a semi-infinite linear chain of Pt atoms. The surface

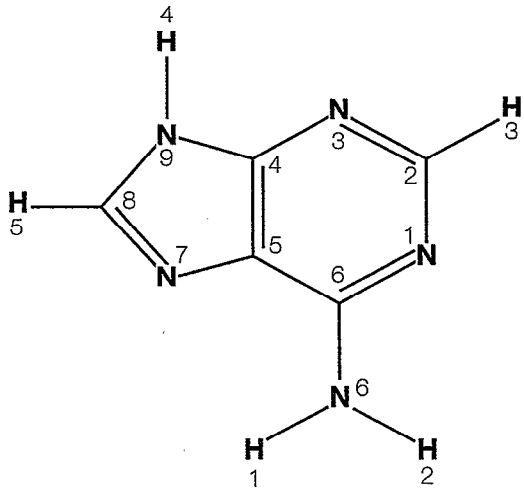

FIG. 1. Structure of adenine showing the numbering system used in the present paper.

properties used for graphite, such as the wave functions and Fermi surface needed to calculate $\Delta_{a,0}$ in Eq. (5) for $\rho_{a,0}$, were those obtained earlier.[16]

The energy zero is chosen to be that of the electron at infinity. Since the work function of graphite is 4.7 eV, the Fermi level of the the graphite is then chosen to be -4.7 eV. The calculated energy value for the HOMO of adenine is then replaced by the negative of the experimental ionization potential for adenine (-7.8 eV), and the other energy levels of the adenine are shifted according to the calculated energy differences between those levels and the HOMO. The energy of the HOMO of adenine (the 25th orbital) relative to the LUMO (the 26th orbital), calculated by the extended Hückel method,[17] is -3.4 eV. Using the corrected energy of -7.8 eV for the HOMO, that for the LUMO is then -4.4 eV. The corrected energy levels for the level immediately below the HOMO and two levels immediately above the LUMO are at -7.9, -4.1, and -3.3 eV, respectively. The Fermi level is -4.7 eV. Thus the LUMO and the LUMO+1 are closest to the Fermi level, according to these estimates.

The separation distance between the adenine plane and the underlying graphite plane does not appear to be known from experiment. However, the x-ray diffraction study of benzene adsorbed on graphite surface reveals that the molecules of benzene lie flat upon the graphite surface at a distance very similar to the interplanar spacing of graphite, 3.35 Å.[18] Theoretical calculations of structures of benzene, naphthalene, and anthracene adsorbed on the basal plane of graphite indicate that the distance between the adsorbate and the underlying graphite does not vary much (only increases slightly) as the number of aromatic rings in the adsorbate molecules increases.[19] Since the adsorption energies of heterocycles appear to be fairly similar to aromatic molecules of the same type,[20] reflecting a similar type of adsorption, we shall presume the same to be true for the distance. For adenine with two aromatic rings, a value of 3.35 Å for the distance is used in the present work, and several results for 3.20 and 3.50 Å are given for comparison. (There will be seen to be little difference in the relative results.)

We consider next the shift of the energy levels due to the physical adsorption. While the adsorption energy for the adenine on graphite does not appear to be available from experiment, the energies of adsorption of substances with aromatic rings, such as benzene and naphthalene, on a graphite surface have been measured experimentally, and are about 0.4 and 0.6 eV, respectively,[21] If we regard the energy as roughly contributed by all 11 C and N atoms of adenine, via van der Waals' dispersion forces, the individual molecular orbitals for those atoms could be regarded as roughly shifted downward by 0.05 eV each. In the absence of a detailed analysis of the adsorption energy, we shall simply suppose that this correction is within the "noise level" of the uncertainty of the energies of the molecular orbitals a of the isolated adenine molecule relative to the Fermi level of the system. Accordingly, we shall use those values for the $\epsilon_a+\Lambda_{a,0}$ in Eq. (5). Had there been a substantial charge transfer interaction instead, a different approach would have been required.

In the present calculations orbitals 24 to 28 of the adenine molecule and 90 carbon atoms of the graphite are included in the calculation of the matrix elements $\langle\phi_a|H|d_m^t\rangle$ appearing in Eq. (8) for the STM current. (In treating the properties of graphite, a solid of infinite area, semi-infinite in the direction normal to the surface, was used in the present work.[16]) In the case of adenine, only the p_z orbitals of the carbon and nitrogen atoms are present in the orbitals 25 to 28.

The present results changed little by adding more molecular orbitals and more graphite carbon atoms to the calculation. A Pt tip is moved over each adenine atom with a fixed value of the current, using a particular assumed position of an adenine molecule. In order to maintain a constant current, the tip is raised or lowered over the different adenine atoms. In a gray scale picture of a constant-current STM image, atoms associated with smaller tip heights correspond to relatively darker spots, and we will refer below to atoms associated with high and low tip heights as bright and dark, respectively.

B. Constraints on possible orientations or positions

We first recall that the structure of graphite consists of planes of carbon atoms, each formed from hexagons. Half of the carbons (α atoms) are located directly above each other in adjacent layers, while the other half (β atoms) are located above the center of the hexagon in the adjacent layers. Each α (β) atom has only β (α) atoms as its nearest neighbors. Mainly the β atoms are detected by STM.[22] Since the six and five membered rings of adenine are approximately similar in shape and size to the graphite hexagons, adenines might have been expected to stack above the graphite in an $\alpha\beta\alpha\beta$-type manner[15] (Fig. 3). We return to this point later.

It was shown in Ref. 15 that the adenine molecules form highly organized lattices following deposition on a heated graphite surface. The adenine molecules appear in lamellae, each lamella consisting of one pair of parallel rows of the adenine molecules. To illustrate the lattice dimensions and

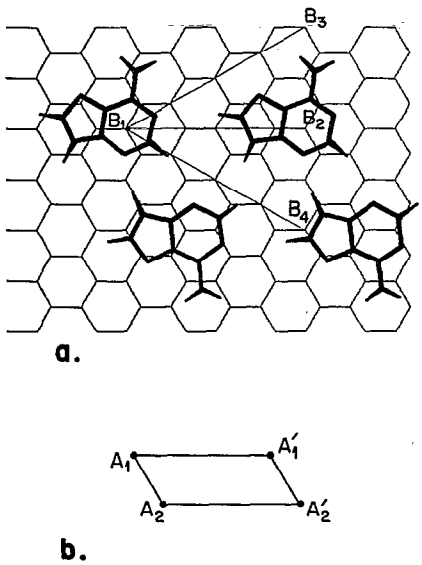

FIG. 2. (a) A periodic bimolecular array of adenine with respect to the graphite lattice obtained in Ref. 15; (b) The lattice unit cell of adenine molecule in a lamella. Points A_i and $A_i'(i = 1,2)$ denote an adenine molecule, respectively.

the arrangement of adenine molecules with respect to the graphite surface, we redraw Fig. 1(d) of Ref. 15 as Fig. 2(a). Some of the β atoms, the points $B_i(i=1,2,3,4)$ are shown as examples in Fig. 2(a). Accordingly, lines B_1B_3 and B_1B_4 pass through other β atoms on the graphite plane and intersect at a 60° angle. Rows of adenine molecules are denoted by horizontal lines, such as the one passing through points B_1 and B_2, and are parallel to each other. They occur only in pairs in the STM pattern,[15] presumably due to the protruding NH_2 group, which prevents in each lamella a close packing of more than two parallel lines of adenines [Fig. 2(a)].

Adenine molecules are denoted by A_i and $A_i'(i = 1,2)$ in Fig. 2(b), which gives the lattice unit cell of two adenine molecules in a lamella on graphite. The STM pattern revealed the following constraints on any molecular model of the structure of the two rows of adenine molecules:[15] (1) Each line of adenine molecules is parallel to a line passing through the β graphite atoms B_1 and B_2 in Fig. 2(a). That line, which in the diagram is shown as roughly passing through the centers of the rings of the adenine molecules, forms an angle of 30° with the lines B_1B_3 and B_1B_4. (2) The A_1A_2 and A_1A_1' in Fig. 2(b) distances are about 5.8 and 8.8 Å, and the angles $\angle A_1'A_1A_2$ and $\angle A_1A_2A_2'$ are 60° and 120°, respectively. These constraints limit somewhat the choice of molecular models of the geometry of the adenine molecule relative to the graphite lattice, but not very much. We explore below whether the calculated STM pattern is or not sensitive to the remaining considerable uncertainty in structure. A sensitivity would mean that a more precise experimental determination of the positions of the adenine molecules with respect to the β atoms of the graphite plane would be needed for a better comparison between theory and experiment. We discuss this point later.

The stacking in which the adenine would stack above the graphite in the $\alpha\beta\alpha\beta$-type manner mentioned earlier is illustrated for a single adenine molecule in Fig. 3. In this orientation atoms C_2, C_4, C_6, and N_7 have graphite atoms roughly below them (namely, the α graphite atoms, which have carbon atoms immediately below them), and other adenine atoms (N_1, N_3, N_8, and C_5) in the rings are roughly above the centers of the hexagons on the graphite plane. However, a close packed array containing this structure would appear to violate a STM-based condition mentioned earlier: The line of the adenine molecules passing through the centers of the rings of adenine forms an angle of 60°, rather than 30°, with the two other lines passing through the β atoms.

Molecular modeling in Ref. 15, beginning with the structure in Fig. 3 led, instead, to a periodic bimolecular array of the structure given in Fig. 2(a), a structure which satisfied the conditions mentioned earlier. We have calculated an STM pattern for this latter structure, and have also calculated the sensitivity of the pattern to translations in the structure, translations which are also consistent with the cited constraints. For example, a systematic translation of the pair of rows of the adenine molecules along the horizontal direction in Fig. 2(a) is not restricted by the above constraints but could be restricted by other STM observations not made in Ref. 15. The effect of various translations on the STM image is examined in Sec. III D.

C. Calculated STM images of adenine molecules based on the two independent positions in Fig. 2(a)

Calculations were first performed for adenine molecules A_1 and A_2 in Fig. 2(a), whose positions were obtained in Ref. 15, as noted earlier, by molecular modeling. In the present calculation a single adenine was placed on graphite, so neglecting the effect of adenine–adenine interactions on the STM pattern at a fixed position of the adenine molecule. The calculated tip heights over each atom are given in Table I for a particular current, the same current being used throughout the present work. The absolute value of the current is discussed later.

In Table I all atoms below the second dashed line appear in the experiments as dark, in the gray scale picture (cf. discussion in Ref. 15). A "†" attached to a hydrogen atom indicates that the experimental result for that atom was not

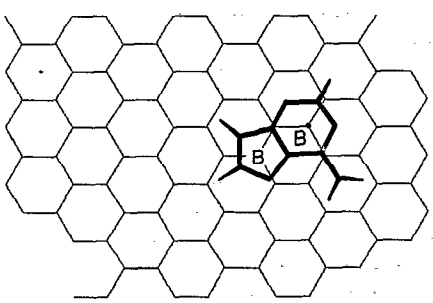

FIG. 3. The structure of adenine with respect to graphite surface used as a starting structure in the molecular modeling performed in Ref. 15.

TABLE I. Tip heights over all adenine atoms in the constant current mode using the two orientations in Ref. 15. A_1 and A_2 below denote structures in Fig. 2.[a,b]

Atom	Tip height (Å) A_1	A_2
N_1	6.35	6.39
C_2	6.58	6.67
N_3	6.26	6.36
C_4	6.32	6.39
C_5	6.32	6.42
C_6	6.50	6.53
C_8	6.61	6.61
$H_3^{\dagger}$	6.42	6.51
$H_4^{\dagger}$	5.78	5.80
$H_5^{\dagger}$	6.45	6.45
N_6	6.13	6.15
N_7	6.20	6.23
N_9	6.31	6.32
H_1	5.77	5.80
H_2	5.77	5.80

[a]In these calculations a graphite–adenine distance of 3.35 Å was used.
[b]All atoms below the second dashed line were not visible in the experimentally observed STM image in Ref. 15. The status of the atoms denoted by † was not specified in Ref. 15.

specifically stated there. The presently calculated results for both orientations A_1 and A_2 are not quite consistent with the experimental findings: For the A_1 structure shown in Fig. 2(a), the N_6 and N_7 atoms do indeed have lower tip heights, as in the experiment, but the height of the remaining dark N atom, N_9, is higher than that of the N_3 atom and hardly distinguishable from that of the bright atoms N_3, C_4, and C_5. For the A_2 molecule although the N_6, N_7, and N_9 atoms correspond to low tip heights or the dark spots among the carbon and nitrogen atoms, the difference in the tip height between N_3 and N_9 is very small (0.04 Å).

In the two rows of adenine molecules in each lamella in Fig. 1(c) of Ref. 15, a comparison of the various positions in Fig. 1 there shows that one row is better resolved than the other. The better resolved images [A_2 and A_2' in the present Fig. 2(b)] correspond to those of the adenine molecules in the lower row in Fig. 1(d) there. The following STM calculations are described in terms of translational shifts of the A_2 in the present Fig. 2(b).

D. Calculated STM images of adenine molecules for other positions

For comparison with the above results, calculations of the STM images were performed for translations of the position of the adenine molecule A_2 with respect to the underlying graphite surface. The displacement was subject to the loose constraints on the adenine lattice noted earlier. To illustrate the discussion, a single A_2 adenine molecule on graphite surface is depicted in Fig. 4. The B's on the graphite lattice in Fig. 4 denote some of the β carbon atoms of the graphite plane. Structures were calculated for ten equally spaced translations along the x axis from right to left in Fig. 4 over a span of one period in length, 4.26 Å. S_i denotes the

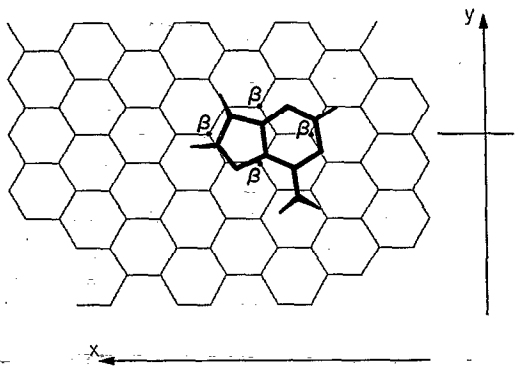

FIG. 4. A single A_2 adenine molecule in Fig. 2(a) with respect to the graphite surface.

structure produced by a translation of A_2 by a distance of $i\times 0.426$ Å, S_1 being depicted in Fig. 5. Calculated tip heights over each atom for these structures are summarized in Table II and in Figs. 6 and 7 for the constant current.

The result for structure S_1 (the structure obtained in Fig. 5 by a translation of only 0.426 Å of the A_2 in Fig. 4) agrees with the available STM findings:[15] For S_1, the tip heights for the N_6, N_7, and N_9 atoms are at least 0.15 Å lower than those for other bright carbon and nitrogen atoms (Table II). From Eq. (8) the STM current also depends, via $\rho_{a,0}$, on the separation between adenine and graphite. Results for a change of the adenine–graphite separation distance are given for the A_2 structure in Table III.

In the present calculations, the results in Figs. 6 and 7 are seen to change smoothly with a translation along the horizontal axis. Since the experimentally measured tip heights were not reported in Ref. 15 (no gray scale calibration was given), a quantitative comparison of the corrugation for Fig. 5 with the experimental STM image cannot be made. However, the differences between the dark and bright atoms in the experiment were estimated[23] to be about 0.1 to 0.2 Å.

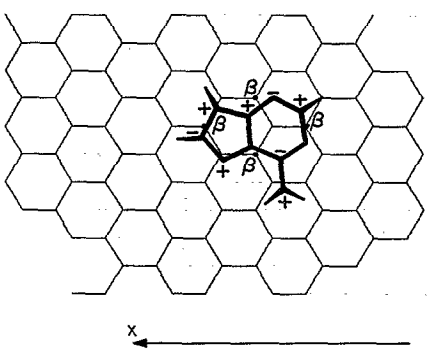

FIG. 5. The position of adenine molecule after a translation of 0.426 Å of the A_2 position from right to left in Fig. 4, to form structure S_1.

TABLE II. Tip heights (Å) over all adenine atoms in the constant current mode. $S_i (i=1-9)$ below denote structures corresponding to a translation of A_2 by an amount of $i\times 0.426$ Å.[a]

	Tip height								
Atom	S_1	S_2	S_3	S_4	S_5	S_6	S_7	S_8	S_9
N_1	6.34	6.39	6.55	6.66	6.69	6.63	6.39	6.38	6.39
C_2	6.70	6.67	6.69	6.78	6.85	6.84	6.67	6.57	6.56
N_3	6.41	6.36	6.29	6.35	6.46	6.48	6.36	6.22	6.21
C_4	6.40	6.40	6.49	6.59	6.62	6.58	6.40	6.32	6.33
C_5	6.45	6.43	6.46	6.54	6.60	6.58	6.43	6.31	6.32
C_6	6.43	6.53	6.73	6.85	6.87	6.79	6.53	6.54	6.56
C_8	6.41	6.60	6.87	6.98	6.99	6.90	6.60	6.66	6.68
H_3^+	6.51	6.28	6.53	6.64	6.71	6.70	6.51	6.40	6.40
H_4^+	5.67	5.81	6.05	6.17	6.18	6.09	5.81	5.83	5.85
H_5^+	6.44	6.17	6.73	6.85	6.86	6.76	6.44	6.51	6.53
N_6	6.03	6.15	6.37	6.48	6.49	6.41	6.15	6.17	6.19
N_7	6.14	6.23	6.43	6.53	6.55	6.47	6.23	6.24	6.26
N_9	6.19	6.32	6.55	6.67	6.68	6.60	6.32	6.36	6.37
H_1	5.64	5.79	6.05	6.14	6.15	6.07	5.79	5.83	5.85
H_2	5.68	5.81	6.02	6.14	6.15	6.08	5.81	5.82	5.84

[a]In these calculations a graphite–adenine distance of 3.35 Å was used. The translation is from right to left.

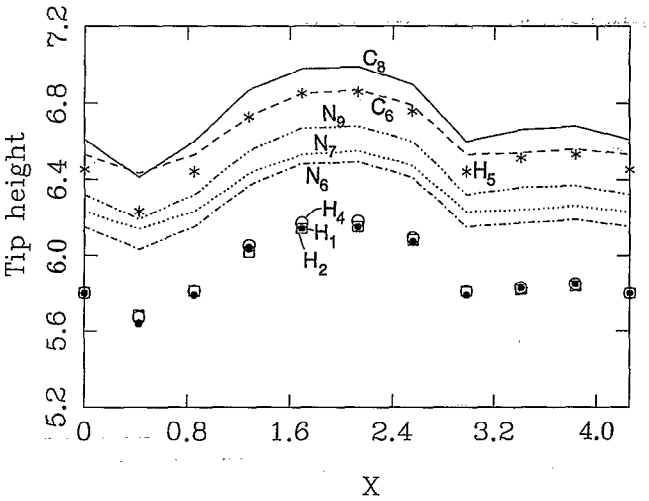

FIG. 7. Variation of the tip heights over the atoms in the adenine molecule with respect to ten equally spaced translations of the A_2 structure over a span of one period of 4.26 Å along the x axis from right to left. The symbols for the various atoms are as follows: □=H_1, ●=H_2, ○=H_4, ∗=H_5, ----=C_6, -·-=N_6, ···=N_7, —=C_8, -···-=N_9.

Equally importantly, it would be useful to determine experimentally the registry of the arrays of adenine with respect to the bright (β) atoms of the graphite surface.

Several of the results in Tables I and II and in Figs. 6 and 7 are the following:

(1) As a whole, the adenine molecule shows a significant dependence of the tip height on the displacement x, being typically largest at $x\simeq 2.0$ Å and least at $x\simeq 0.4$ Å.
(2) Certain atoms show a fairly large variation in tip heights with x, approximately between 0.4 and 0.6 Å (C_6,C_8,N_6,N_7,N_9,H_1,H_2,H_4,H_5) and some show a more modest variation (C_2,C_4,C_5,N_1,N_3,H_3). The first group of atoms shows more or less parallel behavior for tip height as a function of x.
(3) For S_5, the brightest atoms are C_2, C_6, C_8, and H_3, while the darkest are N_3, H_1, H_2, and H_4.
(4) For S_1, the brightest atoms are C_2 and H_3, while the darkest are N_7, N_9, H_1, H_2, and H_4.

We shall attempt to explain or interpret some of these results with the following suggestions, which we shall also attempt to document:

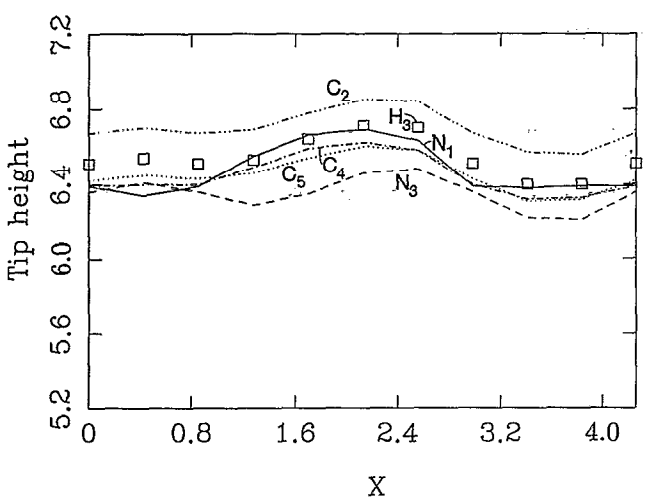

FIG. 6. Variation of the tip heights over the atoms in the adenine molecule with respect to ten equally spaced translations of the A_2 structure over a span of one period of 4.26 Å along the x axis from right to left. The symbols for the various atoms are as follows: —=N_1, -·-·-=C_2, ----=N_3, □=H_3, -·-=C_4, ···=C_5.

TABLE III. Tip heights over all adenine atoms in the constant current mode for structure A_2.[a]

Atom	Tip height (Å) $D=3.35$	Δh $D=3.20$	Δh $D=3.50$
N_1	6.39		
C_2	6.67		−0.01
N_3	6.36	−0.01	
C_4	6.39		−0.01
C_5	6.42		−0.02
C_6	6.53	0.01	−0.01
C_8	6.61		−0.02
H_3^+	6.51	0.01	−0.02
H_4^+	5.80	0.02	−0.04
H_5^+	6.45	0.01	−0.03
N_6	6.15		
N_7	6.23		
N_9	6.32		
H_1	5.80	0.01	−0.03
H_2	5.80	0.01	−0.02

[a]D is the adenine–graphite distance, and Δh is the change in tip height relative to that for $D=3.35$ Å when D is changed to the indicated value. A blank in the column indicates no change.

TABLE IV. The local density of states $\rho_{a,0}$ ($\times 10^4$ eV^{-1}) of the molecular orbital a for structures S_1 and S_5.[a]

	S_1			S_5		
a	$\rho_{a,0}$	$\rho^-_{a,0}$	$\rho^+_{a,0}$	$\rho_{a,0}$	$\rho^-_{a,0}$	$\rho^+_{a,0}$
24	0.0032	−2.0964	2.0996	0.0073	−2.1707	2.1780
25	0.3914	−6.6028	6.9941	0.2128	−6.6481	6.8609
26	2.6130	−927.7629	930.3699	39.3980	−907.4473	946.7540
27	7.6762	−218.8846	226.5567	4.9488	−219.4928	224.4390
28	0.6112	−45.9139	46.5250	0.8187	−45.7170	46.5356

[a]$\rho^-_{a,0}$ and $\rho^+_{a,0}$ denote the negative and positive parts of $\rho_{a,0}$, respectively. In these calculations a graphite–adenine distance of 3.35 Å was used.

(i) The large variation in mean tip height for the adenine molecule with x [points (1) and (2) above] is primarily due to a change in relative importance of M.O. 26 and 27 (LUMO and LUMO+1) with x. This change appears to be due, at least in part, to the different sign distribution of the atomic coefficients in these two orbitals, the energies of the M.O.'s relative to the Fermi level, and to the different proximity of the various adenine atoms to, particularly, the β atoms of the lattice, thereby affecting a delicate cancellation of large positive and negative contributions to $\rho_{a,0}$ in Eq. (8) and hence to the current.

(ii) The behavior of the tip height for the individual H atoms is primarily due to that of the atoms to which they are attached.

(iii) The dominance of an atom such as C_2 at all x, reflects, in part, its large coefficients in both M.O. 26 and 27. However, the behavior of an atom depends also, in part, on the coefficients of its neighbors and, in some cases, its next nearest neighbors.

For completeness we also show in Figs. 9 and 10 the effect of successive y displacements of structure A_2 over a unit period in the lattice. The magnitudes of the effects there are comparable to those seen in the x displacements, and we focus our discussion on the latter.

To consider some of the points (1)–(4), we first note that from Eq. (8) each molecular orbital contributes to the STM current through its local density of states $\rho_{a,0}$ and its interaction matrix element with the tip orbitals: A larger $\rho_{a,0}$ results in a larger contribution to the STM current, and $\rho_{a,0}$ depends upon the position of the adenine molecule with respect to the graphite surface. The essence of an interpretation based on Eqs. (5)–(10) is as follows.

TABLE VI. Atomic coefficients in the LUMO and LUMO+1 of adenine.[a]

Atom	LUMO (M.O. 26)	LUMO+1 (M.O. 27)
N_1	0.0583	−0.5544
C_2	0.4041	0.7675
N_3	−0.4083	−0.2491
C_4	0.2838	−0.3659
C_5	0.0325	0.3869
C_6	−0.5163	0.1932
C_8	−0.6489	0.1381
$H_3^\dagger$	0.0000	0.0000
$H_4^\dagger$	0.0000	0.0000
$H_5^\dagger$	0.0000	0.0000
N_6	0.2940	−0.1092
N_7	0.3454	−0.2665
N_9	0.2238	0.1025
H_1	0.0000	0.0000
H_2	0.0000	0.0000

[a]Each coefficient is for the p_z orbital of the corresponding atom. Coefficients for other atomic orbitals are zero in the above molecular orbitals. The normalization of the coefficients c_i is the usual one, $\Sigma^N_{i,j} c_i c_j S_{ij} = 1$, where S_{ij} is the overlap integral for atomic orbitals on atoms i and j.

For all the calculations in the present paper, the calculated $\rho_{a,0}$'s for the LUMO (M.O. 26) and LUMO+1 (M.O. 27) are seen in Tables IV and V to be far greater than those for other orbitals, because the LUMO and LUMO+1 are closer in the present calculation to the Fermi level of the graphite. As a result, the calculated STM pattern is largely determined by those two orbitals.

In Table IV, M.O. 26 is seen to have the dominant $\rho_{a,0}$ at S_5, while M.O. 27 is seen to be dominant at S_1. This change is seen in Table IV to arise from changes in cancellation between the positive ($\rho^+_{a,0}$) and negative ($\rho^-_{a,0}$) contributions to $\rho_{a,0}$ rather than in marked changes in the $\rho^+_{a,0}$ and $\rho^-_{a,0}$ themselves. At first glance, it might seem surprising that the $\rho^+_{a,0}$ (and $\rho^-_{a,0}$) are much larger for M.O. 26 than for M.O. 27: The c_i's that appear in both orbitals have more or less comparable magnitude (Table VI) but are situated on different atoms. The source of the difference in, say, $\rho^+_{26,0}$ and $\rho^+_{27,0}$ lies in the different values of the energy denominators in Eq. (5) for the two M.O.'s. The $\epsilon_a + \Lambda_{a,0}$ there is estimated to be about 0.6 eV (=−4.1+4.7 eV) for M.O. 27 and 0.3 eV

TABLE V. The local density of states $\rho_{a,0}$ ($\times 10^4$ eV^{-1}) of the molecular orbital a for structures A_2 and S_i (i=2–4 and 6–9).[a]

					$\rho_{a,0}$			
M.O.	A_2	S_2	S_3	S_4	S_6	S_7	S_8	S_9
24	0.0008	0.0063	0.0078	0.0078	0.0059	0.0063	0.0017	0.0005
25	0.2639	0.3118	0.1514	0.1138	0.2622	0.3118	0.0224	0.0644
26	7.2451	6.8360	22.8439	38.2880	26.3481	6.8360	9.6469	10.4337
27	5.3837	5.4651	1.5433	1.1336	7.8040	5.4651	2.1878	1.8694
28	0.4540	0.7633	0.8543	0.8788	0.6827	0.7633	0.3690	0.3498

[a]In these calculations a graphite–adenine distance of 3.35 Å was used. The results for S_1 and S_5 are given in Table IV.

TABLE VII. Values for $\Delta_{a,0}$ ($\times 10^4$ eV) of the molecular orbital a for structures S_1 and S_5.[a]

M.O.	S_1 $\Delta_{a,0}$	$\Delta^-_{a,0}$	$\Delta^+_{a,0}$	S_5 $\Delta_{a,0}$	$\Delta^-_{a,0}$	$\Delta^+_{a,0}$
24	0.0320	−21.4664	21.4994	0.0747	−22.2279	22.3026
25	3.7614	−63.4527	67.2141	2.0453	−63.8886	65.9339
26	0.2352	−83.5634	83.7986	3.5458	−81.7309	85.2767
27	2.7634	−78.8121	81.5755	1.7816	−79.0311	80.8127
28	1.1979	−89.9951	91.1929	1.6047	−89.6090	91.2137

[a]$\Delta^-_{a,0}$ and $\Delta^+_{a,0}$ denote the negative and positive parts of $\Delta_{a,0}$, respectively. In these calculations a graphite–adenine distance of 3.35 Å was used.

(=−4.4+4.7 eV) for M.O. 26, according to the present calculations. The $\Delta_{a,0}$ in the denominator there is much smaller than these energies ($\sim 10^{-2}$ eV, as noted in Table VII), and so the denominator is $(\epsilon_a+\Lambda_{a,0})^2$. Indeed, each $\Delta^+_{a,0}$ is seen in Table VII to be more or less comparable for S_1 and S_5, as is $\Delta^-_{a,0}$, as expected.

The atom H_3, which is attached to C_2, is seen from Fig. 6 to be "bright," and its brightness changes relatively little with x. Inasmuch as the c_i for H_3 in both S_1 and S_5 is very small (Table VI), the current when the tip is over H_3 is due to the proximity of the tip to C_2, which has a high coefficient in M.O. 26 and 27 and is bright at both S_1 and S_5. H_3 tracks C_6 in Fig. 6. Similarly, H_1 and H_2, which have zero coefficients in M.O. 26 and 27 (Table VI) are seen in Fig. 7 to track N_6 to which they are attached, and owe "their current," when the tip is over them, to the proximity of the tip to N_6. N_6 is much darker on the average than C_2, and so H_1 and H_2 are much darker on the average than H_3. For the same reason, H_4, which is attached to N_9, is seen in Fig. 6 to track the latter, while H_5, which is attached to C_8, is like C_8, relatively bright (Fig. 7) and also tracks the latter. We comment on the relative brightness for the C and N atoms for a given structure, such as S_5, later.

A next question is why the adenine molecule as a whole tends to be bright in the S_5 position and relatively dark in the S_1 structure: The net $\rho_{a,0}$ for any M.O. a is the result of positive and negative contributions, but it itself is positive [Eq. (5)], and so is $\Delta_{a,0}$ [Eq. (6)]. The negative contributions to $\Delta_{a,0}$ arise from products of c_i's and c_j's in Eq. (9) which have opposite signs. If an atom is close to a β atom it will contribute more to $\Delta_{a,0}$, because the solid–adsorbate matrix element is larger. If the atom has a negative c_i with nearby positive c_i atoms, there will tend to be more cancellation in $\Delta_{a,0}$. (However, the c_i^2 term is also enhanced, so there are opposing effects.) If, instead, it is close to an α atom, its negative contribution to $\Delta_{a,0}$ will be somewhat smaller, resulting in less cancellation and so in a brighter adenine.

Such an argument offers one suggestion why $\Delta_{26,0}$ is smaller for structure S_1 than for S_5: The atomic coefficients for M.O. 26 and 27 were listed in Table VI. The signs "+" and "−" in Figs. 5 and 8 denote the positive and negative coefficients in the LUMO of adenine (M.O. 26), respectively, while the atoms without a sign assigned in those figures have a negligible coefficient. In part because of the proximity of C_8 to a β atom in S_1 it is seen that in structure S_1 the negative contribution $\rho^-_{26,0}$ to $\rho_{26,0}$ is larger than that in S_5, and so

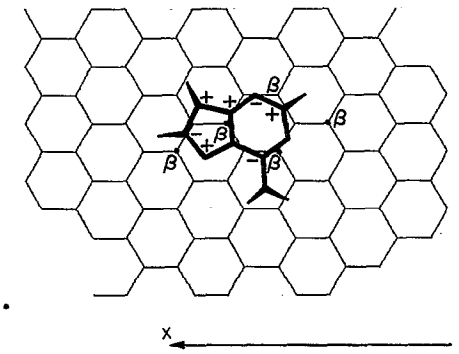

FIG. 8. The position of adenine molecule after a translation of 2.13 Å of the A_2 position along the x axis from right to left, to form structure S_5.

there is more cancellation in S_1, and $\Delta_{26,0}$ becomes small.[24] However, since each $\Delta_{a,0}$ is seen in Table VII to be a small difference between two large quantities, such an argument has some uncertainty.

While the behavior of the individual H's was understandable, as described above, the behavior for the individual C and N atoms is somewhat less transparent. As an example, we consider S_5, where M.O. 26 is dominant, and examine Table II for tip heights, using Table VI for the M.O. coefficients. Among the carbon atoms, C_8, C_6, and C_2 have relatively large coefficients and are bright. However, C_5 and C_4 have very different coefficients, C_5's being very small, and yet they have comparable tip heights, though not as high as those of C_8, C_6, and C_2. Among the N's, N_1 has the smallest coefficient but is the brightest, or one of the two brightest N atoms for structure S_5. The nearest neighbors will be seen

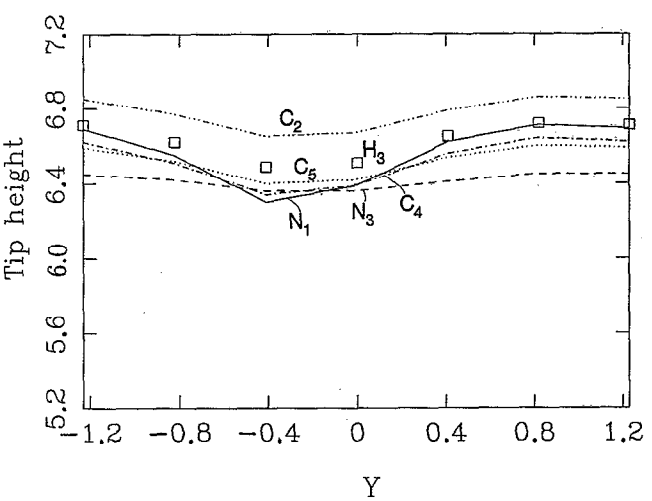

FIG. 9. Variation of the tip heights over the atoms in the adenine molecule with respect to six equally spaced translations of the A_2 structure over a span of one period of 2.46 Å along the y axis from zero to 1.23 Å and from zero to −1.23 Å. The symbols for the various atoms are the same as those in Fig. 6.

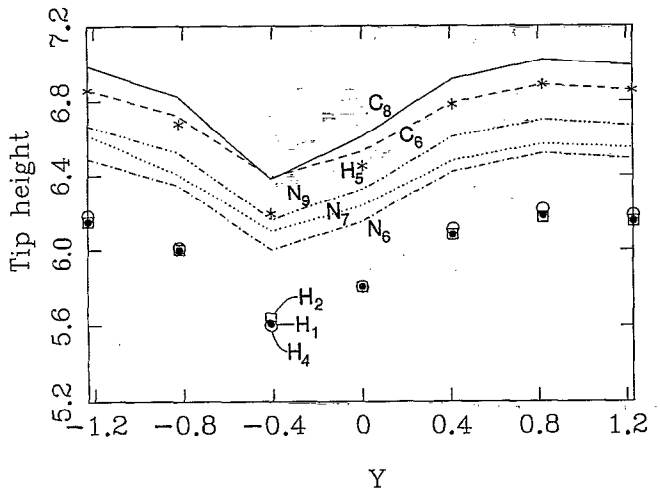

FIG. 10. Variation of the tip heights over the atoms in the adenine molecule with respect to six equally spaced translations of the A_2 structure over a span of one period of 2.46 Å along the y axis from zero to 1.23 Å and from zero to −1.23 Å. The symbols for the various atoms are the same as those in Fig. 7.

later (Table IX) to have a large effect on the tip height for N_1.

In the case of the H's, we saw that the tip height was determined not by the H's (whose coefficients were zero) but by that of atoms to which those H's are attached. Similarly, the tip height for a C or an N atom is determined not only (or even mainly in some cases) by the interaction of that atom with the tip but also by the interaction of the tip with nearby atoms. We explore this question next. We first note from Table VIII, using S_5 and M.O. 26 and 27 as an example, that the squares of the matrix elements in Eq. (10) are not small

TABLE VIII. Values for $V_a \equiv \Sigma_m |\langle \phi_a | H | d_m^t \rangle|^2$ ($\times 10^2$ eV) in Eq. (10) for the M.O. 26 and 27 for structure S_5.[a]

Atom	M.O.=26 V_a	M.O.=26 V_a^-	M.O.=26 V_a^+	M.O.=27 V_a	M.O.=27 V_a^-	M.O.=27 V_a^+
N_1	1.10	−2.38	3.48	1.04	−6.12	7.16
C_2	0.85	−1.22	2.07	3.05	−3.18	6.23
N_3	0.59	−8.62	9.21	4.89	−12.62	17.51
C_4	0.94	−5.20	6.14	1.48	−6.11	7.59
C_5	0.82	−6.69	7.51	2.49	−7.06	9.55
C_6	1.14	−1.54	2.68	6.27	−1.98	2.61
C_8	1.21	−1.08	2.28	0.06	−0.32	0.38
H_3^t	0.86	−0.44	1.30	3.01	−1.38	4.38
H_4^t	1.16	−3.38	4.54	0.34	−1.04	1.38
H_5^t	1.21	−0.43	1.64	0.06	−0.07	0.13
N_6	1.17	−3.31	4.48	0.39	−1.15	1.54
N_7	1.14	−5.78	6.92	0.38	−3.49	3.87
N_9	1.18	−3.32	4.50	0.27	−1.43	1.70
H_1	1.19	−3.35	4.54	0.18	−0.92	1.10
H_2	1.16	−3.90	5.06	0.37	−1.16	1.53

[a]In these calculations the tip heights over different atoms were those in Table II for structure S_5. V_a^- and V_a^+ denote the negative and positive parts of V_a, respectively.

TABLE IX. Dependence of tip height (Å) on nearest neighbors and next nearest neighbors, for S_5.[a]

Atom	Height (full)[b]	Height n.n.n[c]	Height (n.n)[d]	Height (atom)[e]
N_1	6.69	6.70	6.75	6.37
C_2	6.85	6.85	6.88	6.97
N_3	6.46	6.51	6.53	6.68
C_4	6.62	6.62	6.75	6.78
C_5	6.60	6.60	6.76	6.38
C_6	6.87	6.86	6.93	7.01
C_8	6.99	6.99	7.02	7.11
N_6	6.49	6.52	6.54	6.53
N_7	6.55	6.54	6.64	6.61
N_9	6.68	6.68	6.73	6.44

[a]Only the C and N atoms are listed.
[b]Full means that all atomic coefficients c_i's are present.
[c]n.n.n means that the c_i's of all atoms but the atom itself, its nearest neighbors and its next nearest neighbors are set equal to zero. The next nearest neighbor refers to the atom which is two bonds away. For example, the next nearest neighbors of N_1 in Fig. 1 are N_3, H_3, C_5, and N_6.
[d]n.n means that the c_i's of all atoms but the atom itself and its nearest neighbors are set equal to zero. For example, the nearest neighbors of atom N_1 in Fig. 1 are C_2 and C_6.
[e]Atom means that the c_i's of all atoms but the atom itself are set equal to zero.

differences between large quantities, and so there is a reasonable expectation that they may be fairly readily interpreted.

To this end, we give in Table IX the tip height for an atom (1) with all coefficients in Eq. (10) present, (2) when the c_i's of all atoms but those of the atom itself are set equal to zero, (3) when the c_i's of all atoms but those of the atom itself and of its nearest neighbors are set equal to zero, and (4) when the c_i's of all but those of the atom itself, its nearest neighbors and its next nearest neighbors are set equal to zero. The results in Table IX are for structure S_5, where M.O. 26 is dominant (Table IV).

We can test in the above way whether the tip heights for the C's and N's in adenine are determined largely by the atom, or by the atom plus its neighbors or whether its next nearest neighbors also play a major role. It is seen in Table IX for S_5 that the heights in which all coefficients c_i but those of the atom, its neighbors and its next nearest neighbors are set equal to zero in Eq. (10) are virtually the same as those in which no coefficients in Eq. (10) are set equal to zero. In many cases it is seen that only an atom and its nearest neighbors make a significant contribution in Eq. (10), but in others (C_4 and C_5 particularly) the next nearest neighbors also contribute significantly. As seen in Fig. 1, C_4 and C_5 are the atoms with the largest number of nonhydrogenic next nearest neighbors. Tip heights in which only the atom's coefficient c_i in Eq. (10) is nonzero (last column in Table IX) are usually quite different from these in which all c_i's in Eq. (10) are given their actual values, but the brightest atoms (C_8, C_6, and C_2) are the brightest in both cases.

For comparison with the results in Tables I and II using molecular orbitals 24–28, calculations were also made for the A_2 and S_1 structures using only the HOMO and LUMO orbitals of the adenine, and the results are given in Table X: It is seen from a comparison with Tables I and II that the results for some of the atoms do not agree with the more

TABLE X. Tip heights over all adenine atoms in the constant current mode using only the HOMO and LUMO orbitals of the adenine for structures A_2 and S_1.[a]

Atom	Tip height (Å) A_2	S_1
N_1	6.27	6.02
C_2	6.35	6.10
N_3	6.01	5.85
C_4	6.19	6.01
C_5	6.19	6.08
C_6	6.45	6.22
C_8	6.59	6.34
$H_3^{\dagger}$	6.16	5.87
$H_4^{\dagger}$	5.71	5.40
$H_5^{\dagger}$	6.43	6.15
N_6	6.11	5.91
N_7	6.17	5.99
N_9	6.28	6.04
H_1	5.77	5.56
H_2	5.76	5.55

[a]In these calculations a graphite–adenine distance of 3.35 Å was used.

complete results, and so other orbitals were needed in the calculation. For adenine the LUMO+1 orbital, for example, is very close to the LUMO in energy and is seen in Table IV to contribute sometimes significantly to the current.

We consider next the assumption made in proceeding from Eq. (3) to Eq. (8), namely, that of "nonoverlapping resonances." Values of the molecular energy levels of the adenine ($a=24$ to 28) are -7.9, -7.8, -4.4, -4.1, and -3.3 eV. The spacing between the energies of the important orbitals, 26 and 27, is 0.3 eV, which is far greater that any of the calculated $2\Delta_{a,0}$'s values listed in Table VII. The latter are typically estimated there to be about 10^{-4} eV. We turn next to the validity of the order of the magnitude of this calculated value of $\Delta_{a,0}$ and, thereby, of the current.

In the constant current calculations presented above, only the relative current was given, and so the constant factor preceding the sum in Eq. (8) was not used. The absolute value for the current in the present approximation is estimated next, to see if it is consistent with the small values of $\Delta_{a,0}$ given above. As an approximation, it is assumed that in Eq. (8) the μ equals α, and β is taken to be 0.69 eV.[25] A bias voltage v of 0.274 V was used in the experiment.[15] It is noted that Eq. (8) is valid for only small v, where the current I is linearly proportional to v. The scanning tunneling spectroscopy or the dependence of I on v for the present system of adenine adsorbed on graphite was not reported in the experiment. For the present system it will be supposed that the use of Eq. (8) for a voltage of 0.274 V also provides a rough estimate of the current. The calculated current based on Eq. (8) is 1.5 nA, which is fortuitously close to the experimental value of 0.7 nA. The adenine–tip separation distance used, as noted earlier, 3.35 Å for this estimated absolute value of the current. The calculation indicates that the very small values of $2\Delta_{a,0}$ listed in Table VII are consistent with the magnitude of the observed current. On that basis, the present assumption of nonoverlapping resonances would be valid.

IV. CONCLUDING REMARKS

The STM image of an adsorbate is related in the present theoretical model to both the tip–adsorbate matrix elements and to an *effective* local density of states at the adsorbate, a density which incorporates the substrate–adsorbate interaction. In applying the present expression to the STM image of adenine adsorbed on a graphite surface, it was found that the tip height of some atoms is relatively independent of the position of the adenine relative to the graphite lattice. The calculations themselves should of course, be regarded as tentative, because of the various approximations used: (1) extended Hückel theory for the molecule, plus tight binding for the solid, (2) perturbation theory for the tip–adsorbate interaction, (3) an approximate estimate of the difference in the energy of the adsorbate orbitals relative to the Fermi energy of the solid, (4) neglect of subtleties of tip–solid electric fields on the energy levels of adsorbate, and (5) the restriction of the calculations to STM at the Fermi level. Condition (5) will be removed in a later paper, in which the STM spectroscopy is given, namely, a calculation of $d \ln I/d \ln V$. This derivative will become a maximum when a resonance is encountered, and then assumption (2) might need to be modified. The maximum STM current for v volts, based on a Landauer expression,[26] is $(2e^2/h)v$, which is about 20 μA for the 0.274 V used in the present paper. This current exceeds by many orders of magnitude the present current of 1.5 nA, and so perturbation theory for the tip–adsorbate/solid calculation appears to be valid.

While some results were insensitive to the position of the adenine molecule on the graphite lattice, others were not: Even the order of bright vs dark was changed for some atoms (Figs. 6 and 7). Thus to make a better comparison between theory and experiment for the latter atoms, a more precise knowledge of the position of the individual adsorbate molecules relative to the substrate lattice is needed. Two ways of doing this are mentioned in Ref. 24, one being to compare the STM pattern for the adsorbate present with that with some of it removed.[27] Another is to vary the bias voltage:[28,29] For alkanes on graphite, for example, a change of tip bias voltage from 0.15 to 0.25 V was reported to change the pattern from that of graphite to another quite different shape, believed to be the adsorbate. Even moirè patterns have been observed, due to interference between the contributions from the substrate and the adsorbate.[28]

In the case of graphite, it would be helpful if the intersection lines of the β atoms mentioned in Sec. III B could be determined relative to that of an adenine molecule. Another factor whose study would be helpful in comparisons of STM experiment and calculations is that of bias voltage, and we are planning such calculations. With increasing bias voltage the α atoms of the graphite lattice are expected to play a larger role.[30] One may anticipate that two effects will occur: The relative importance of molecular orbitals 26 and 27, as well as of other orbitals may change and, equally importantly, the relative importance[30] of the β and α graphite atoms will change. It is possible, for example, that the observation in other experiments of seeing the equilateral triangular pattern of the β atoms at low-bias voltages and observing a different adsorbatelike behavior at higher bias

voltage is due in part to a decreasing importance of the β atoms at higher biases. However, to treat properly such an experimental observation we expect that it will be necessary to use a method[31] which treats the tails of the graphite and tip wave functions, and hence of a direct graphite–tip interaction, more accurately than does the tight binding approximation.

ACKNOWLEDGMENTS

It is a pleasure to acknowledge the support of this research by the Office of Naval Research, the National Science Foundation, and by the International Joint Research Program of NEDO (Japan). We are also pleased to acknowledge use of the resources of the JPL/Caltech CRAY Supercomputer.

[1] For example, G. Binnig, H. Rohrer, Ch. Gerber, and E. Weibel, Phys. Rev. Lett. **49**, 57 (1982); **50**, 120 (1983).
[2] For example, D. M. Eigler and E. K. Schweizer, Nature (London) **344**, 524 (1990); E. Kopatzki and R. J. Behm, Surf. Sci. **245**, 255 (1991).
[3] For recent reviews, see, for example (a) X. Gao and M. J. Weaver, Ber. Bunsenges. Phys. Chem. **97**, 507 (1993); (b) J. Frommer, Angew. Chem. Int. Ed. Engl. **31**, 1298 (1992); J. P. Rabe, *ibid.* **28**, 117 (1989).
[4] For a review, see N. D. Lang, Comments Condens. Matter. Phys. **14**, 253 (1989).
[5] D. M. Eigler, P. S. Weiss, E. K. Schweizer, and N. D. Lang, Phys. Rev. Lett. **66**, 1189 (1991).
[6] P. H. Lippel, R. J. Wilson, M. D. Miller, Ch. Wöll, and S. Chiang, Phys. Rev. Lett. **62**, 171 (1989).
[7] S. Ohnishi and M. Tsukada, Solid State Commun. **71**, 391 (1989).
[8] E. Kopatzki, G. Doyen, D. Drakova, and R. J. Behm, J. Microsc. **151**, 687 (1988).
[9] T. R. Coley, W. A. Goddard III, and J. D. Baldeschwieler, J. Vac. Sci. Technol. B **9**, 470 (1991).
[10] P. Sautet and C. Joachim, Chem. Phys. Lett. **185**, 23 (1991); Surf. Sci. **271**, 387 (1992). This approach is a nonperturbative one.
[11] J. W. Mintmire, J. A. Harrison, R. J. Colton, and C. T. White, J. Vac. Sci. Technol. A **10**, 603 (1991).
[12] H. Ou-Yang, B. Källebring, and R. A. Marcus, J. Chem. Phys. **98**, 7565 (1993).
[13] (a) D. M. Newns, Phys. Rev. **178**, 1123 (1969); (b) P. W. Anderson, *ibid.* **124**, 41 (1961); (c) see also U. Fano, *ibid.* **124**, 1866 (1961).
[14] For a review, cf. J. P. Muscat and D. M. Newns, Prog. Surf. Sci. **9**, 1 (1978).
[15] M. J. Allen, M. Balooch, S. Subbiah, R. J. Tench, W. Siekhaus, and R. Balhorn, Scanning Microsc. **5**, 625 (1991).
[16] H. Ou-Yang, B. Källebring, and R. A. Marcus, J. Chem. Phys. **98**, 7405 (1993).
[17] R. Hoffmann, J. Chem. Phys. **39**, 1397 (1963).
[18] I. Gameson and T. Rayment, Chem. Phys. Lett. **123**, 150 (1986).
[19] C. Bondi, P. Baglioni, and G. Taddei, Chem. Phys. **96**, 277 (1985).
[20] P. B. Dallakyan and R. S. Petrova, Russ. J. Phys. Chem. **61**, 1640 (1987).
[21] E. H. M. Wright and A. V. Powell, J. Chem. Soc., Faraday 1 **68**, 1908 (1972).
[22] For example, G. Binnig, H. Fuchs, Ch. Gerber, H. Rohrer, E. Stoll, and E. Tosatti, Europhys. Lett. **1**, 31 (1985).
[23] M. J. Allen (private communication).
[24] For M.O. 26, the contribution of C_8 to $\rho_{26,0}$ in structure S_1 was 3.79, which is comparable with the 2.60 for $\rho_{26,0}$ in Table IV. For S_5, the contribution of C_8 to $\rho_{26,0}$ was 13.80, which is about 1/3 of the value for S_5 in Table IV.
[25] Y. Boudeville, J. Rousseau-Violet, F. Cyrot-Lackmann, and S. N. Khanna, J. Phys. (Paris) **44**, 433 (1983).
[26] A survey of recent references on this maximum is given in C. W. J. Beenakker and H. van Hunter, Solid State Phys. **44**, 1 (1991), pp. 110 ff; cf. N. D. Lang, Phys. Rev. B **36**, 8173 (1987); J. H. Schott and H. S. White, in press.
[27] D. P. E. Smith, J. K. H. Hörber, G. Binnig, and H. Nejoh, Nature (London) **344**, 641 (1990).
[28] J. P. Rabe, S. Buchholz, and L. Askadskaya, Synthetic Metals **54**, 339 (1993); cf. S. Buchholz and J. P. Rabe, J. Vac. Sci. Technol. B **9**, 1126 (1991).
[29] K. Yackoboski, Y. H. Yao, G. C. McGonigal, and D. J. Thomson, Ultramicroscopy **42**, 963 (1992).
[30] An increasing importance of the α atoms with bias voltage is reported in D. Tomanek, S. G. Louie, H. J. Mamin, D. W. Abraham, R. E. Thomson, E. Ganz, and J. Clarke, Phys. Rev. B **35**, 7790 (1987).
[31] cf. J. Tersoff, in *Scanning Tunneling Microscopy and Related Methods*, edited by R. J. Behm, N. Garcia, and H. Rohrer (Kluwer, Dordrecht, 1990), p. 77ff. We have made calculations in which the direct interaction between the graphite atoms and the tip was included, and found negligible effect on the current. Calculations with wave functions having improved tails may be needed to match the low bias results obtained in Refs. 28 and 29.